Articles

Chain Termination and Transfer Reactions in the Acrylate Polymerization by a Monometallic Chiral Zirconocenium Catalyst System

Wesley R. Mariott, Antonio Rodriguez-Delgado, and Eugene Y.-X. Chen*

Department of Chemistry, Colorado State University, Fort Collins, Colorado 80523-1872

Received October 26, 2005; Revised Manuscript Received December 15, 2005

ABSTRACT: Unlike the living polymerization of methacrylates and acrylamides by the monometallic propagating, chiral *ansa*-zirconocenium ester enolate *rac*-(EBI)Zr^+(THF)[OC(O^{i}Pr)═CMe_2][$MeB(C_6F_5)_3$]$^-$ [**1**; EBI = $C_2H_4(Ind)_2$], the polymerization of acrylates such as *n*-butyl acrylate (*n*-BA) by **1** proceeds in an uncontrolled fashion to only moderate monomer conversions, producing poly(*n*-BA) with three types of chain structures—one major linear and two minor cyclic *β*-ketoester-terminated poly(*n*-BA) chains. The combined polymerization, chain structure, and model reaction studies have shown the presence of substantial chain termination processes in this system that prevent it from achieving high monomer conversions and producing only the living linear chain structure. The proposed overall three-step mechanism, involving isomerization of the cyclic reactive intermediate, backbiting cyclization to eliminate an alcohol, and chain termination by the alcohol, explains the catalyst deactivation pathways as well as the resulting polymer chain structures. Chain transfer reactions involving acidic α-protons are insignificant as compared to backbiting cyclizations involving the activated antepenultimate ester group of the growing polymer chain, which is the chief catalyst deactivation pathway for the current monometallic catalyst system.

Introduction

Since the initial discovery of metallocene-based systems for the polymerization of alkyl methacrylates,[1] particularly methyl methacrylate (MMA), with a patent disclosure by Farnham and Hertler[1c] in 1988 as well as two independent journal publications by Yasuda et al.[1b] and Collins and Ward[1a] in 1992, the field has attracted increasing attention due to the demonstrated remarkable versatility of these systems in terms of catalyst structures and polymerization characteristics. The polymerization of alkyl methacrylates mediated by group 4 metallocene and related complexes, including achiral zirconocenes,[2] chiral *ansa*-zirconocenes,[3] achiral titanocenes,[1c,4] chiral *ansa*-titanocenes,[5] half-sandwich titanium complexes,[6] and constrained geometry titanium and zirconium complexes,[7] has been extensively and computationally[8] studied. When used in suitable initiating complex forms (e.g., metallocene ester enolates), these systems are living, allowing for control over polymer number-average molecular weights (M_n) and molecular weight distributions (MWD = M_w/M_n)[2b,g,k] as well as the synthesis of well-defined block copolymers.[2h,3a,f,7a] A high degree of control over polymer tacticity[3,7] and the production of stereoblock P(MMA)[3d,g] are also possible using appropriate chiral metallocene complexes.

While the polymerization of alkyl methacrylates by group 4 metallocene and related complexes has been extensively investigated and considerable success achieved,[1−8] reports on the polymerization of alkyl acrylates—that contain an active α-proton as opposed to a methyl group in methacrylates—by these systems are scarce, and only limited success has been met. Soga and Deng[9] employed a three-component system consisting of *rac*-(EBI)$ZrMe_2$/[Ph_3C][$B(C_6F_5)_4$]/$MeAl(BHT)_2$ [EBI = $C_2H_4(Ind)_2$; BHT = 2,6-di-*tert*-butyl-4-methylphenoxy] for the polymerization of the sterically hindered *tert*-butyl acrylate (*t*-BA), affording P(*t*-BA) with moderate to broad MWDs (M_w/M_n = 1.23−2.20) in low to moderate polymer yields (6−60%) with extended reaction times (17−24 h). Collins and co-workers[2k] investigated the polymerization of the unhindered *n*-butyl acrylate (*n*-BA) by a two-component bimetallic system consisting of the well-defined catalyst [Cp_2Zr^+Me(THF)][BPh_4]$^-$ and initiator Cp_2ZrMe[OC(O^{t}Bu)═CMe_2]; a monomer conversion of 55% and a polymer MWD of M_w/M_n = 2.02 were observed for the polymerization at 0 °C in a [*n*-BA]/[initiator] ratio of ∼100, with higher conversions and lower polymer MWDs being achieved only at lower polymerization temperatures. This process is not living, and analysis of the low-molecular-weight P(*n*-BA) by matrix-assisted laser desorption/ionization time-of-flight mass spectroscopy (MALDI−TOF MS) led to two proposed modes of chain termination processes, the predominate of which involves the backbiting cyclization of the growing polymer chain. Most recently, a third report on the polymerization of acrylates (*t*-BA and *n*-BA) by Hadjichristidis et al. appeared,[10] which employed Soga's three-component systems, including $Cp_2ZrMe_2/B(C_6F_5)_3/ZnEt_2$, *rac*-(EBI)$ZrMe_2/B(C_6F_5)_3/ZnEt_2$, and *rac*-(EBI)$ZrMe_2$/[$HNMe_2Ph$]-[$B(C_6F_5)_4$]/$ZnEt_2$; the polymer yields obtained from these polymerizations of *n*-BA and *t*-BA for 24 h did not exceed 30 and 32%, respectively, in any case, regardless of the catalyst

* Corresponding author. E-mail: eychen@lamar.colostate.edu.

10.1021/ma052305+ CCC: $33.50
Published on Web 01/24/2006

system or polymerization conditions employed. The results from the above three reports clearly indicate the presence of considerable chain termination processes in the polymerization of α-proton-containing acrylates by group 4 metallocene complexes; this observation is in sharp contrast to the isoelectronic, neutral organolanthanide complexes such as $(C_5Me_5)_2SmMe(THF)$ which mediate the living polymerization of alkyl acrylates.[11] However, the polymerization of acrylates using a well-defined single-component, chiral monometallic propagating zirconocenium ester enolate system, which has been shown to behave similarly to lanthanocenes, serving as both catalyst and initiator for the polymerization of methacrylates,[3a,b] has not been experimentally investigated[12] and is the focus of this current contribution.

We have recently elucidated mechanisms for the polymerizations of alkyl methacrylates[3a,b] and acrylamides[13] mediated by the well-defined, single-component chiral *ansa*-zirconocenium ester enolate complex, *rac*-(EBI)Zr^+(THF)[OC(O^{i}Pr)=CMe$_2$]-[MeB$(C_6F_5)_3]^-$ (**1**). Our combined studies of synthesis, polymerization, kinetics, as well as polymer microstructures and chain structures have shown that the polymerization of methacrylates and acrylamides by **1** proceeds in a living fashion through a monometallic, enantiomorphic site-control mechanism, affording the corresponding highly isotactic polymers. The objective of the current study was to investigate the polymerization of acrylates using this well-defined chiral, monometallic propagating zirconocenium ester enolate system. To this end, we have studied the polymerization of *n*-BA by **1** in detail, obtained unambiguous evidence for chain termination reactions occurring in this polymerization that prevent high monomer conversions, as well as elucidated the mechanism of these reactions that are responsible for the overall catalyst deactivation.

Experimental Section

Materials and Methods. All syntheses and manipulations of air- and moisture-sensitive materials were carried out in flamed Schlenk-type glassware on a dual-manifold Schlenk line, a high-vacuum line, or in an argon-filled glovebox. NMR-scale reactions were conducted in Teflon-valve-sealed J. Young-type NMR tubes. HPLC grade organic solvents were sparged with nitrogen during filling of the solvent reservoir and then dried by passage through activated alumina (for THF and CH_2Cl_2) followed by passage through Q-5-supported copper catalyst (for toluene and hexanes) stainless steel columns. Benzene-d_6 and toluene-d_8 were dried over sodium/potassium alloy and filtered before use, whereas $CDCl_3$ and CD_2Cl_2 were dried over activated Davison 4 Å molecular sieves. NMR spectra were recorded on either a Varian Inova 300 (FT 300 MHz, ^{1}H; 75 MHz, ^{13}C; 282 MHz, ^{19}F) or a Varian Inova 400 spectrometer. Chemical shifts for ^{1}H and ^{13}C spectra were referenced to internal solvent resonances and are reported as parts per million relative to tetramethylsilane, whereas ^{19}F NMR spectra were referenced to external $CFCl_3$.

n-Butyllithium (1.6 M in hexanes), diethyl malonate (DEM), diisopropylamine, 2,6-di-*tert*-butyl-4-methylphenol (butylated hydroxytoluene, BHT-H), ethyl acetoacetate (EAA), lithium dimethylamide, methyl isobutyrate (MIB), and zirconium tetrachloride were purchased from Aldrich Chemical Co., trimethylaluminum (neat) from Strem Chemical Co., methyllithium (1.6 M in diethyl ether) from Acros, and dimethyl malonate (DMM), dimethyl succinate (DMS), di-*tert*-butyl malonate (DBM), and trimethylsilyl trifluoromethanesulfonate (TMSOTf) from Alfa Aesar. These reagents were used as received, except for the following reagents that were further treated or purified: the amine was degassed using three freeze−pump−thaw cycles; BHT-H was recrystallized from hexanes; all esters including DBM, DEM, DMM, DMS, EAA, and MIB were purified by first degassing and drying over CaH_2 overnight, followed by vacuum distillation and stored over activated Davison 4 Å molecular sieves inside the glovebox.

Methyl methacrylate (MMA) was purchased from Aldrich Chemical Co. and purified by first degassing and drying over CaH_2 overnight, followed by vacuum distillation; final purification of MMA involved titration with neat tri(*n*-octyl)aluminum to a yellow end point[14] followed by a second vacuum distillation. *n*-Butyl acrylate (*n*-BA) was purchased from Acros and purified by first degassing and drying over CaH_2 overnight followed by distillation under reduced pressure. The purified monomers were stored in brown glass bottles over activated Davison 4 Å molecular sieves (for *n*-BA) in a −30 °C freezer inside the glovebox.

Tris(pentafluorophenyl)borane, $B(C_6F_5)_3$, was obtained as a research gift from Boulder Scientific Co. and further purified by recrystallization from hexanes at −30 °C. The $(C_6F_5)_3B$·THF adduct was prepared by addition of THF to a toluene solution of the borane followed by removal of the volatiles and drying in vacuo. Literature procedures were employed for the preparation of the following compounds and metallocene complexes: $(EBI)H_2$ [EBI = $C_2H_4(Ind)_2$],[15] *rac*-(EBI)Zr$(NMe_2)_2$,[16] *rac*-(EBI)ZrMe_2,[16] *rac*-(EBI)Zr^+(THF)[OC(O^{i}Pr)=CMe$_2$][MeB$(C_6F_5)_3]^-$ (**1**).[3a,b]

Modified Synthesis of *rac*-(EBI)ZrMe[OC(O^{i}Pr)=CMe$_2$]. In an argon-filled glovebox, a 50 mL Schlenk flask was equipped with a magnetic stir bar, charged with 0.567 g (1.50 mmol) of *rac*-(EBI)-ZrMe_2 and 30 mL of toluene, capped with a septum, removed from the glovebox, and interfaced to a Schlenk line. The flask was cooled to 0 °C in an ice bath under positive nitrogen pressure before the addition of 1.6 mL (1.6 mmol, 1.0 M in hexanes) TMSOTf via gastight syringe to the above vigorously stirred solution. The reaction mixture was stirred at 0 °C for 1 h before being allowed to warm to ambient temperature and stirred for an additional 21 h. An aliquot of the reaction mixture revealed ∼13% unreacted *rac*-(EBI)ZrMe_2 remaining, and therefore an additional 0.22 mL (0.22 mmol, 1.0 M in hexanes) of TMSOTf was added to the reaction mixture via gastight syringe. The reaction mixture was allowed to stir for an additional 4 h in a warm water bath. The volatiles were removed in vacuo, and the resulting residue was dried before being taken into the glovebox, where the product was extracted into 40 mL of toluene and filtered through a pad of Celite. The filtrate was transferred to a 60 mL reactor and cooled to −30 °C in the freezer of the glovebox before the addition of 0.205 g [1.50 mmol, 1 equiv based on *rac*-(EBI)ZrMe_2] of Me$_2$C=C(O^{i}Pr)OLi to the vigorously stirred solution. The reaction mixture was allowed to gradually warm to ambient temperature and stirred for 24 h before being filtered through a pad of Celite. The volatiles of the filtrate were removed in vacuo, and the resulting yellow powder was dried, affording 0.665 g [90%, based on *rac*-(EBI)ZrMe_2] of the spectroscopically pure title complex. The spectroscopic data are the same as those reported in the literature.[3b]

Isolation of the Initiation (Single *n*-BA Addition) Product of 1: *rac*-(EBI)Zr^+[OC(O^{n}Bu)=CHCH$_2$C(Me$_2$)C(O^{i}Pr)=O][MeB-$(C_6F_5)]^-$ (2). In an argon-filled glovebox, a 30 mL glass reactor was charged with 29.5 mg (0.060 mmol) of *rac*-(EBI)ZrMe[OC-(O^{i}Pr)=CMe$_2$], 35.0 mg (0.060 mmol) of $(C_6F_5)_3B$·THF, and 10 mL of CH_2Cl_2; this solution was allowed to stir for 10 min at ambient temperature, cleanly generating **1**.[3a] To this in situ generated and vigorously stirred CH_2Cl_2 solution of **1** was added 8.6 μL (0.060 mmol) *n*-BA at ambient temperature. The color of the resulting mixture changed instantaneously from dark orange to light orange. The solution was allowed to stir for 30 min at ambient temperature before the volatiles were removed in vacuo, yielding a sticky light orange solid. The crude product was washed with 5 × 2 mL hexanes and dried in vacuo to give 62.0 mg (91%) of the title complex as an orange powder. The spectroscopic data of the isolated product are the same as those obtained by the in situ generation method listed as follows, except for the absence of signals for THF, which was removed upon drying of the isolated product. Anal. Calcd for $C_{53}H_{44}BF_{15}O_4Zr$: C, 56.24; H, 3.92. Found: C, 56.16; H, 3.82.

^{1}H NMR (CD_2Cl_2, 23 °C) for *rac*-(EBI)Zr^+[OC(O^{n}Bu)=CHCH$_2$C-(Me$_2$)C(O^{i}Pr)=O][MeB$(C_6F_5)]^-$ (generated in situ): δ 8.16 (d, J = 8.7 Hz, 1H), 7.85 (d, J = 8.7 Hz, 1H), 7.38−7.09 (m, 6H), 5.94 (d, J = 3.0 Hz, 1H), 5.83 (d, J = 3.0 Hz, 1H), 5.61 (d, J = 3.0 Hz, 1H), 5.44 (d, J = 3.0 Hz, 1H), 4.61 (sept, J = 6.3 Hz, 1H,

OC*H*Me$_2$), 4.31−4.03 (m, 2H, CH_2CH$_2$), 3.92−3.78 (m, 2H, CH$_2$CH_2), 3.74 (s, br, 4H, α-CH_2, free THF derived from **1**), 2.15 (d, J = 15.0 Hz, 1H, CH_2), 1.88−1.82 (m, 1H, CH_2; 4H, β-CH_2, free THF), 1.69−1.56 (m, 2H, OCH$_2$CH_2CH$_2$CH$_3$), 1.43−1.31 (m, 2H, OCH$_2$CH$_2$CH_2CH$_3$), 1.38 (d, J = 6.3 Hz, 3H, OCH*Me*$_2$), 1.25 (s, 3H, C*Me*$_2$), 1.20 (d, J = 6.3 Hz, 3H, OCH*Me*$_2$), 1.18 (s, 3H, C*Me*$_2$), 0.94 (t, J = 7.5 Hz, 3H, OCH$_2$CH$_2$CH$_2$CH_3), 0.49 (s, br, 3H, B*Me*). The proton signals for OCH_2CH$_2$CH$_2$CH$_3$ and =C*H* could not be assigned with confidence due to overlap with other peaks. ^{19}F NMR (CD$_2$Cl$_2$, 23°C): δ −131.50 (d, $^3J_{F-F}$ = 20.0 Hz, 6F, *o*-F), −163.64 (t, $^3J_{F-F}$ = 20.3 Hz, 3F, *p*-F), −166.20 (m, 6F, *m*-F).

Generation of *rac*-(EBI)Zr$^+$(THF)(O^{t}Bu)[MeB(C$_6$F$_5$)]$^-$ (3). An authentic sample (**3**) of cationic zirconocene *tert*-butoxide complexes[17] was prepared using modified literature procedures.[17a] In an argon-filled glovebox, a 25 mL Schlenk flask was loaded with *rac*-(EBI)ZrMe$_2$ (200 mg, 0.530 mmol) and 15 mL of toluene; the flask was sealed with a septum, removed from the glovebox, and suspended in a 23 °C water bath. A 5 mL toluene solution of ^{t}BuOH (70.7 mg, 0.954 mmol) was added to the above stirred solution via a gastight syringe. The reaction was stirred at 23 °C for 1.3 h before the volatiles were removed in vacuo. The resulting light yellow powder was dried in vacuo, affording 140 mg (73%) of *rac*-(EBI)ZrMe(O^{t}Bu). Next, the isolated *rac*-(EBI)ZrMe(O^{t}Bu) (7.3 mg, 0.02 mmol) was mixed with an equimolar amount of (C$_6$F$_5$)$_3$B·THF (11.7 mg, 0.02 mmol) in 0.7 mL of CD$_2$Cl$_2$ to cleanly generate the corresponding cationic species (**3**) as a bright yellow homogeneous solution.

^{1}H NMR (CD$_2$Cl$_2$, 23°C) for *rac*-(EBI)ZrMe(O^{t}Bu): δ 7.74 (dd, 1H), 7.44 (dd, 1H), 7.33 (dt, 1H), 7.23 (dt, 1H), 7.12−6.96 (m, 4H), 6.36 (d, J = 3.3 Hz, 1H), 6.30 (d, J = 3.3 Hz, 1H), 6.02 (d, J = 3.3 Hz, 1H), 5.82 (d, J = 3.3 Hz, 1H), 3.63−3.51 (m, 1H, CH_2CH$_2$), 3.49−3.25 (m, 3H, CH_2CH_2), 0.82 (s, 9H, C*Me*$_3$), −1.13 (s, 3H, Zr*Me*). ^{1}H NMR (CD$_2$Cl$_2$, 23 °C) for **3**: δ 8.04−7.99 (m, 1H), 7.88−7.83 (m, 1H), 7.51−7.22 (m, 6H), 6.58 (dd, 1H), 6.41 (d, J = 3.6 Hz, 1H), 6.29−6.23 (m, 2H), 4.00−3.76 (m, 4H, CH_2CH_2), 3.74−3.66 (m, 2H, α-CH_2, THF), 3.49−3.42 (m, 2H, α-CH_2, THF), 2.11−1.82 (m, 4H, β-CH_2, THF), 1.01 (s, 9H, C*Me*$_3$), 0.49 (s, br, 3H, B*Me*). ^{19}F NMR (CD$_2$Cl$_2$, 23°C): δ −131.51 (d, $^3J_{F-F}$ = 21.2 Hz, 6F, *o*-F), −163.61 (t, $^3J_{F-F}$ = 20.3 Hz, 3F, *p*-F), −166.21 (m, 6F, *m*-F).

Generation of *rac*-(EBI)Zr$^+$[OC(Me)=CHC(=O)(OEt)][MeB(C$_6$F$_5$)$_3$]$^-$ (4). In an argon-filled glovebox, to a solution of complex **2** (7.4 mg, 6.5 μmol) in 0.6 mL of CD$_2$Cl$_2$ was added ethyl acetoacetate (0.8 μL, 6.5 μmol) via micropipet, and the resulting mixture was briefly mixed before being transferred to a J. Young-type NMR tube for ^{1}H and ^{19}F NMR analyses. The NMR spectra clearly showed the complete disappearance of both starting materials and are consistent with the formation of the protonolysis product, complex **4**, and the corresponding coproduct ^{n}BuOC(=O)CH$_2$-CH$_2$C(Me$_2$)C(=O)O^{i}Pr.

^{1}H NMR (CD$_2$Cl$_2$, 23 °C) for **4**: δ 7.50−7.05 (m, 8H), 6.87 (m, 1H), 6.65 (m, 1H), 6.25 (m, 1H), 6.03 (m, 1H), 5.38 (s, 1H, =C*H*), 4.21−3.89 (m, 4H, CH_2CH_2), 1.98 (s, 3H, OC*Me*), 0.46 (s, br, 3H, B*Me*). (The O*Et* protons could not be assigned with confidence due to overlap with both ethylene bridging and the coproduct ^{n}BuO peaks.) ^{19}F NMR (CD$_2$Cl$_2$, 23 °C): δ −131.56 (d, $^3J_{F-F}$ = 19.2 Hz, 6F, *o*-F), −163.76 (t, $^3J_{F-F}$ = 20.3 Hz, 3F, *p*-F), −166.33 (m, 6F, *m*-F).

Chain Transfer Model Reactions of 1 with Methyl Isobutyrate and Dimethyl Malonate. In an argon-filled glovebox, to a CD$_2$Cl$_2$ solution of **1** (0.020 mmol) was added 2.3 μL of MIB (0.020 mmol) at ambient temperature. The solution was quickly transferred to a Teflon-valve-sealed J. Young-type NMR tube, and the ^{1}H and ^{19}F NMR were monitored over a 5 h period. The reaction mixture gave NMR spectra consistent with the formation of the protonolysis product *rac*-(EBI)Zr$^+$(L)[OC(OMe)=CMe$_2$][MeB(C$_6$F$_5$)$_3$]$^-$ [**5**, L = isopropyl isobutyrate (PIB), MIB, or THF] as well as the presence of the unreacted starting material in a 1:2 ratio; there was no noticeable change in this ratio after 5 h.

^{1}H NMR (CD$_2$Cl$_2$, 23 °C) for **5**: δ 8.00 (d, J = 8.7 Hz, 1H), 7.96−7.92 (m, 1H, overlapping with **1**), 7.50−7.14 (m, 6H, overlapping with **1**), 6.69 (d, J = 3.3 Hz, 1H), 6.26 (m, 2H), 6.08 (d, J = 3.3 Hz, 1H), 4.15−3.80 (m, 4H, CH_2CH_2, overlapping with **1**), 3.67 (s, 3H, O*Me*), 1.45 (s, 3H, =C*Me*$_2$), 1.35 (s, 3H, =C*Me*$_2$), 0.49 (s, br, 3H, B*Me*). ^{19}F NMR (CD$_2$Cl$_2$, 23°C): δ −131.51 (d, $^3J_{F-F}$ = 20.0 Hz, 6F, *o*-F), −163.55 (t, $^3J_{F-F}$ = 20.3 Hz, 3F, *p*-F), −166.16 (m, 6F, *m*-F).

A similar procedure was followed for the reaction of **1** and DMM, which resulted in a rapid consumption of all starting materials and the appearance of a new set of resonances consistent with the formation of the corresponding protonolysis product, *rac*-(EBI)Zr$^+$[OC(OMe)=CHC(OMe)=O][MeB(C$_6$F$_5$)$_3$]$^-$ (**6**), and the readily identifiable free isopropyl isobutyrate coproduct. ^{1}H NMR (CD$_2$Cl$_2$, 23 °C) for **6**: δ 7.80 (d, J = 8.7 Hz, 2H), 7.70−7.15 (m, 6H), 6.62 (d, J = 3.3 Hz, 2H), 6.26 (d, J = 3.3 Hz, 2H), 4.05−3.29 (m, 4H, CH_2CH_2), 3.43 (s, 6H, O*Me*), 0.49 (s, br, 3H, B*Me*). (The =C*H* proton could not be assigned with confidence due to overlap with other peaks.) ^{19}F NMR (CD$_2$Cl$_2$, 23°C): δ −131.53 (d, $^3J_{F-F}$ = 18.9 Hz, 6F, *o*-F), −163.59 (t, $^3J_{F-F}$ = 20.3 Hz, 3F, *p*-F), −166.19 (m, 6F, *m*-F).

General Polymerization Procedures. Polymerizations were performed either in 30 mL glass reactors inside the glovebox or in 25 mL Schlenk flasks interfaced to a dual-manifold Schlenk line. In a typical procedure, for polymerizations of *n*-BA using the in situ generated **1**, 10.3 mg (20.9 μmol) of *rac*-(EBI)ZrMe[OC(O^{i}Pr)=CMe$_2$] and 12.2 mg (20.9 μmol) of (C$_6$F$_5$)$_3$B·THF were dissolved in 5 mL of CH$_2$Cl$_2$ in a 25 mL Schlenk flask and allowed to stir 10 min at ambient temperature to cleanly generate the cationic zirconocenium ester enolate **1** before being suspended in a preequilibrated bath at the desired temperature. *n*-BA (0.3 mL, 2.09 mmol) was quickly added via gastight syringe, and the sealed flask was kept with vigorous stirring at the bath temperature. After the desired time interval, the polymerization was quenched by the addition of 5 mL of 5% HCl-acidified methanol followed by removal of the volatiles in vacuo and drying in a vacuum oven at 50 °C overnight to a constant weight. Polymer conversions were monitored, either throughout the course of the polymerization or immediately before quenching, by removing 0.2 mL aliquots of the reaction mixture via syringe and quickly quenching into 4 mL vials containing 0.6 mL of undried "wet" CDCl$_3$ stabilized by 250 ppm of BHT-H. The quenched aliquots were analyzed by ^{1}H NMR to obtain conversion data. For NMR scale polymerization runs, *rac*-(EBI)ZrMe[OC(O^{i}Pr)=CMe$_2$] (0.02 mmol) and (C$_6$F$_5$)$_3$B·THF (0.02 mmol) were dissolved in 0.7 mL of CD$_2$Cl$_2$ or toluene-d_8 and allowed to mix for 10 min at ambient temperature before the addition of a predetermined ratio of monomer. These polymerizations were monitored by ^{1}H NMR to obtain conversion data.

For the sequential copolymerization of MMA and *n*-BA, 11.5 mg (23.4 μmol) of *rac*-(EBI)ZrMe[OC(O^{i}Pr)=CMe$_2$] and 13.7 mg (23.4 μmol) of (C$_6$F$_5$)$_3$B·THF were dissolved in 5 mL of CH$_2$Cl$_2$ in a 30 mL glass reactor and allowed to stir 10 min at ambient temperature, generating **1** in situ. MMA (0.5 mL, 4.67 mmol) was quickly added to the vigorously stirred solution of **1** in CH$_2$Cl$_2$ at ambient temperature via a pipet, and the polymerization mixture was allowed to stir for 15 min before the addition of *n*-BA (0.34 mL, 2.34 mmol). The reactor was kept with vigorous stirring at ambient temperature for 30 min before the copolymerization was quenched by the addition of 5 mL of 5% HCl-acidified methanol. The quenched mixture was precipitated into 100 mL of methanol and stirred for 30 min before the polymer was filtered off, washed with methanol, and dried in a vacuum oven at 50 °C overnight to a constant weight.

For the chain transfer polymerization of MMA by **1** using enolizable esters as chain transfer reagents (CTRs), *rac*-(EBI)ZrMe-[OC(O^{i}Pr)=CMe$_2$] (18.7 μmol) and (C$_6$F$_5$)$_3$B·THF (18.7 μmol) were dissolved in 5 mL of CH$_2$Cl$_2$ and allowed to stir 10 min at ambient temperature to generate **1**. A solution of a predetermined ratio of a CTR in MMA (9.35 mmol) was added to the catalyst solution via a pipet, and the polymerization was allowed to stir for 30 min at ambient temperature before being quenched by the

Scheme 1

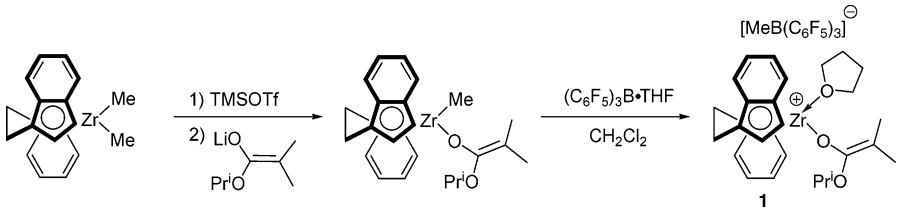

addition of 5 mL of 5% HCl-acidified methanol. The quenched mixture was precipitated into 100 mL of MeOH and allowed to stir for 30 min before the polymer was filtered off, washed with MeOH, and dried in a vacuum oven at 50 °C overnight to a constant weight.

Polymer Characterizations. The low-molecular-weight P(*n*-BA) sample was analyzed by matrix-assisted laser desorption/ionization time-of-flight mass spectroscopy (MALDI−TOF MS); the experiment was performed on an Ultraflex MALDI−TOF mass spectrometer (Bruker Daltonics) operated in reflector mode using a Nd:YAG laser at 355 nm and 25 kV accelerating voltage. A thin layer of a 1% NaI solution was first deposited on the target plate, followed by 1 μL of both sample and matrix (dithranol, 10 mg/mL in THF). Gel permeation chromatography (GPC) analyses of the polymers were carried out at 40 °C and a flow rate of 1.0 mL/min, with $CHCl_3$ as the eluent, on a Waters University 1500 GPC instrument equipped with four 5 μm PL gel columns (Polymer Laboratories) and calibrated using 10 PMMA standards. Chromatograms were processed with Waters Empower software (2002); number-average molecular weight and polydispersity of polymers are given relative to PMMA standards. NMR spectra of the resulting polymers were recorded in $CDCl_3$ and analyzed according to literature procedures.[18]

Results and Discussion

Polymerization of *n*-Butyl Acrylate by 1. The literature route to the chiral *ansa*-zirconocene precatalyst *rac*-(EBI)ZrMe-[OC(O^{i}Pr)═CMe$_2$][3b] was considerably revised to allow for a semi-one-pot approach starting from the zirconocene dimethyl precursor. As can be seen in Scheme 1, the revised synthesis involves the reaction of *rac*-(EBI)ZrMe$_2$ with 1.2 equiv of TMSOTf in toluene followed by removal of the volatiles and drying (to remove any remaining excess TMSOTf) to give *rac*-(EBI)ZrMe(OTf), which was subsequently treated with 1 equiv of Me$_2$C═C(O^{i}Pr)OLi, affording the pure *rac*-(EBI)ZrMe[OC-(O^{i}Pr)═CMe$_2$] in 90% isolated yield (based on *rac*-(EBI)-ZrMe$_2$). This yield is substantially higher than the overall yield of 54% obtained from the previously reported three-step process[3b] involving transformations from *rac*-(EBI)ZrMe$_2$ to *rac*-(EBI)Zr(OTf)$_2$ to *rac*-(EBI)ZrMe(OTf) to *rac*-(EBI)ZrMe-[OC(O^{i}Pr)═CMe$_2$]. The chiral cationic *ansa*-zirconocene ester enolate complex **1** can be either isolated[3b] or cleanly generated in situ by mixing *rac*-(EBI)ZrMe[OC(O^{i}Pr)═CMe$_2$] with $(C_6F_5)_3B$•THF in CH_2Cl_2 at room temperature.[3a] The cation **1** is stable in a solution of CH_2Cl_2 at room temperature; subsequently, the in situ generated **1** in CH_2Cl_2 was used for all polymerization and model reaction studies.

We have previously demonstrated that the methacrylate polymerization by complex **1**, which models the isospecific active propagating species for the methacrylate polymerization, proceeds in a living fashion via a monometallic propagation, enantiomorphic site-control mechanism, enabling the efficient synthesis of highly isotactic homopolymers having narrow MWDs with typical M_w/M_n values of 1.03−1.05 and high initiator efficiencies as well as stereodiblock copolymers with well-defined structures.[3a,b] In sharp contrast, the polymerization of *n*-BA by this well-defined complex is not controlled. Polymerizations of *n*-BA carried out in Teflon-valve-sealed J. Young-type NMR tubes in toluene-d_8 at high catalyst loadings ($[n\text{-BA}]_0/[\mathbf{1}]_0 = 10-20$) proceeded to high conversions (100−92%) within 10 min; as the $([n\text{-BA}]_0/[\mathbf{1}]_0$ ratio increases to 100, the conversions dropped drastically to 40%, even after extended reaction times, with maximum conversions being reached typically within the first 10 min. Preparative-scale polymerizations of *n*-BA in CH_2Cl_2 at 23 °C $\{[n\text{-BA}]_0/[\mathbf{1}]_0 = 25, 50, 100\}$ in the stirred reactors also gave low monomer conversions between 44 and 57% (runs 1−3, Table 1). Kinetic profiling of the polymerization of *n*-BA at $[n\text{-BA}]_0/[\mathbf{1}]_0 = 100$ by ^{1}H NMR analysis of reaction mixture aliquots revealed a maximum conversion of only 47% reached within the first 10 min, with no further conversion after extended polymerization times (run 3). Lowering of the reaction temperature to 0 and −22 °C only slightly increases the maximum conversions to 52% and 63%, respectively (runs 4 and 5). The isolated P(*n*-BA) samples have relatively broad MWDs with M_w/M_n values ranging from 1.26 to 1.51. Additionally, the measured M_n values are considerably higher than the expected M_n values, giving low initiator efficiencies of ≤65%. These results clearly show that the polymerization of *n*-BA by **1** proceeds only to moderate conversions with low to moderate initiator efficiencies in even a low monomer/initiator ratio of $\{[n\text{-BA}]_0/[\mathbf{1}]_0 \leq 100\}$, indicative of the presence of chain termination reactions that prevent high monomer conversions.

Table 1. *n*-BA Polymerization Results by Chiral Zirconocenium Ester Enolate Complex 1[a]

run no.	$[n\text{-BA}]_0/[\mathbf{1}]_0$	time (min)	temp (°C)	conv (%)	10^3M_n[b] (g/mol)	PDI[b] (M_w/M_n)	I*[c] (%)
1	25	10	23	57	4.5	1.27	41
2	50	10	23	44	6.7	1.41	42
3	100	10	23	47	9.2	1.38	65
4	100	10	0	52	14.0	1.51	48
5	100	30	−22	63	12.8	1.26	63

[a] Carried out in CH_2Cl_2 using an external temperature-control bath at the indicated temperatures. [b] Number-average molecular weight (M_n) and polydispersity index (PDI) determined by GPC relative to PMMA standards in $CHCl_3$. [c] Initiator efficiency (I*) = M_n(calcd)/M_n(exptl), where M_n(calcd) = MW(*n*-BA) × $[n\text{-BA}]_0/[\mathbf{1}]_0$ × conversion (%).

Polymer Chain Structures of P(*n*-BA) Produced by 1. Analysis of a low-molecular-weight P(*n*-BA) sample by MALDI−TOF mass spectrometry provided unambiguous evidence for the presence of chain termination/transfer reactions in the polymerization of *n*-BA by **1**. As can be seen in Figure 1, the mass spectrum of the P(*n*-BA) sample consists of one major (**A**) and two minor (**B** and **C**) series of mass ions, with the spacing of the mass ions within each series being that of the mass of the P(*n*-BA) repeat unit (m/z = 128). A plot of m/z values for series **A** in the MALDI−TOF mass spectrum vs the number of *n*-BA repeat units (n) afforded a straight line with a slope of 128.03 and an intercept of 153.34 (Figure 2); the slope corresponds to the mass of the *n*-BA monomer, whereas the intercept is the sum of the masses of Na^+ (from the added NaI) and the chain-end groups which corresponds to a formula of $C_7H_{14}O_2$. This analysis clearly shows that the polymer for series **A** has a structural formula of ^{i}PrOC(═O)C(Me$_2$)−(*n*-BA)$_n$−H,

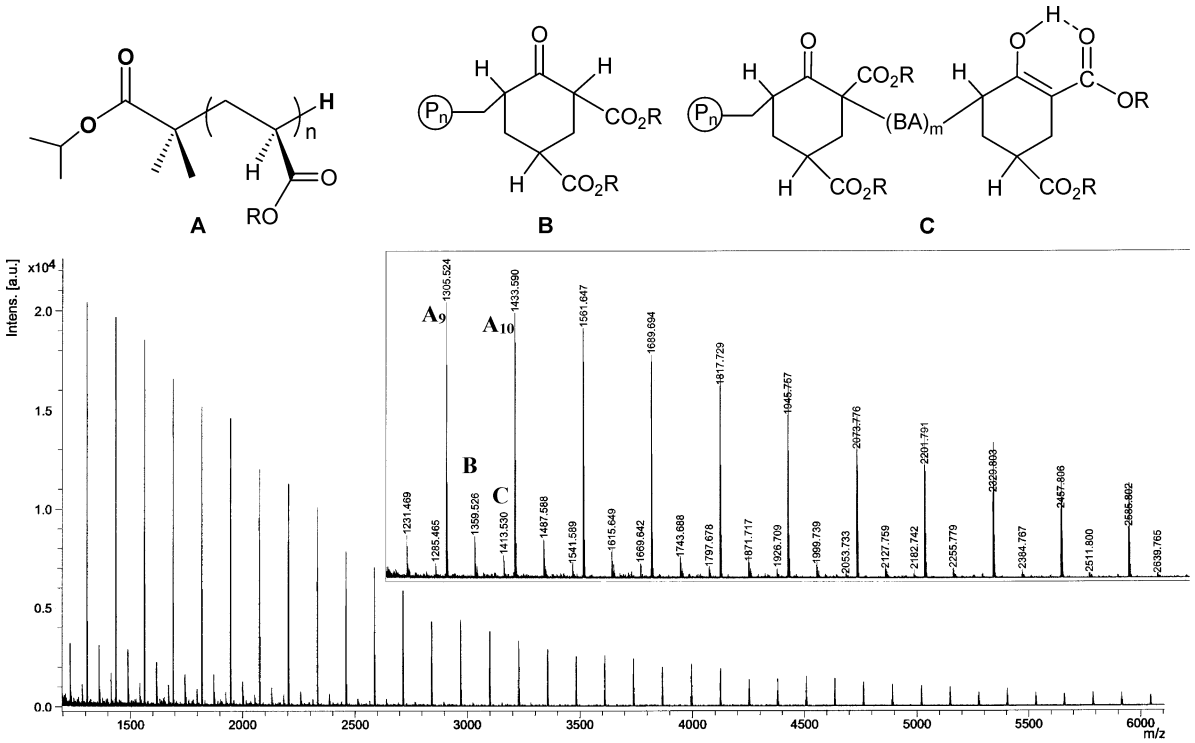

Figure 1. MALDI−TOF mass spectrum of the low-molecular-weight P(*n*-BA) produced by **1** in CH_2Cl_2 at 23 °C (R = ^{n}Bu); the sample was analyzed as quenched without purification.

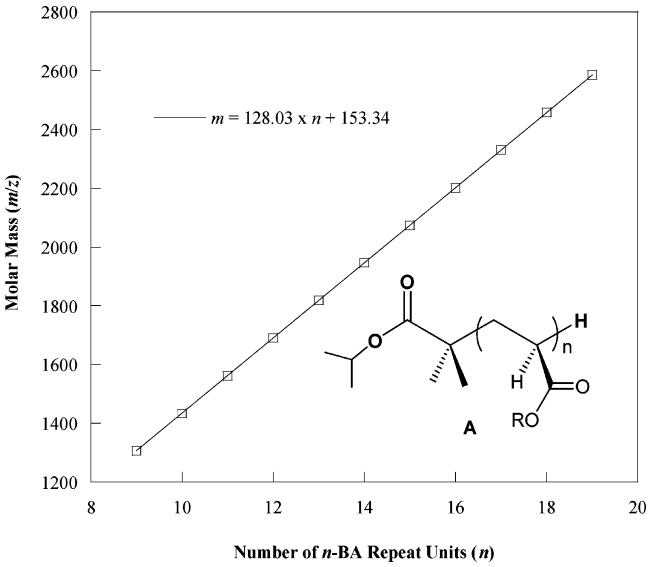

Figure 2. Plot of *m*/*z* values of series **A** from Figure **1** vs the number of *n*-BA repeat units (*n*).

where the initiation chain end [^{i}PrOC(=O)C(Me$_2$)−] is derived from the initiating isopropyl isobutyrate group in complex **1** and the termination chain end (H) from either the acidic workup after the polymerization or a chain termination process during the polymerization (vide infra). Hence, the peaks in series **A** correspond to the linear (living if terminated during the workup) polymer chains produced by complex **1**.

The remaining two minor series of peaks (**B** and **C**) in the MALDI−TOF mass spectrum maintain a respective spacing of mass ions that corresponds to the repeat unit of P(*n*-BA) (*m*/*z* = 128); however, they do not exhibit a linear chain structure similar to **A**. A closer examination of these minor series of mass ions revealed a relationship to the linear polymer chain structure mass ions (series **A**) through the loss of one and two ^{n}BuOH molecules for series **B** and **C**, respectively, resulting in the formation of two corresponding cyclic structures at different stages of the polymerization (vide infra).

Chain Termination Reactions in the Acrylate Polymerization by 1. To examine whether the *n*-BA monomer would decompose catalyst **1** or not, we carried out the stoichiometric reaction of *n*-BA and **1**, which clearly shows the rapid, complete disappearance of the *n*-BA vinyl signals and the appearance of a new set of resonances corresponding to the formation of the single *n*-BA addition (chain initiation) product, *rac*-(EBI)-Zr$^+$[OC(O^{n}Bu)=CHCH$_2$C(Me$_2$)C(O^{i}Pr)=O][MeB(C$_6$F$_5$)]$^-$ (**2**; Scheme 2); analogous single MMA, *N*-isopropylacrylamide, and *N*,*N*-dimethylmethacrylamide addition products have been previously isolated and characterized.[3a,13a] Next, we examined the catalytic competency of species **2** via its isolation and subsequent use for the polymerization of 500 equiv of MMA, which led to quantitative formation of highly isotactic P(MMA) having a narrow MWD (PDI = 1.03), with polymerization characteristics being similar to those obtained directly by **1**. These results clearly indicate a facile initiation process for the polymerization of *n*-BA by **1** via conjugate addition to generate the highly active propagating species **2** and suggest that chain termination reactions must occur during the propagating steps with the growing P(*n*-BA) chain bound to the metal center.

As evidenced by the MALDI−TOF mass spectrum, the polymerization of *n*-BA by **1** produces P(*n*-BA) exhibiting three types of chain structures, for which the mechanism of formation is proposed in Scheme 3. Linear chain structure **A** can be produced by the same mechanism previously established for the polymerization of MMA, which proceeds through the cyclic ester enolate intermediate **D** (resting state);[3a] this is a living process, giving the well-defined living linear chain structure. However, this linear chain structure can also be produced from a chain-termination step involving the reaction between resting intermediate **D** and ^{n}BuOH generated by the backbiting cyclization (vide infra). Cyclic structures **B** and **C** are derived from

Scheme 2

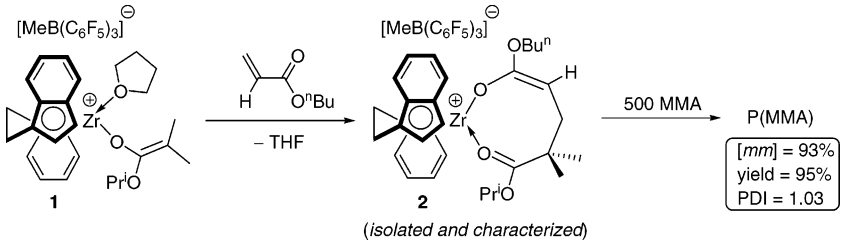

Scheme 3

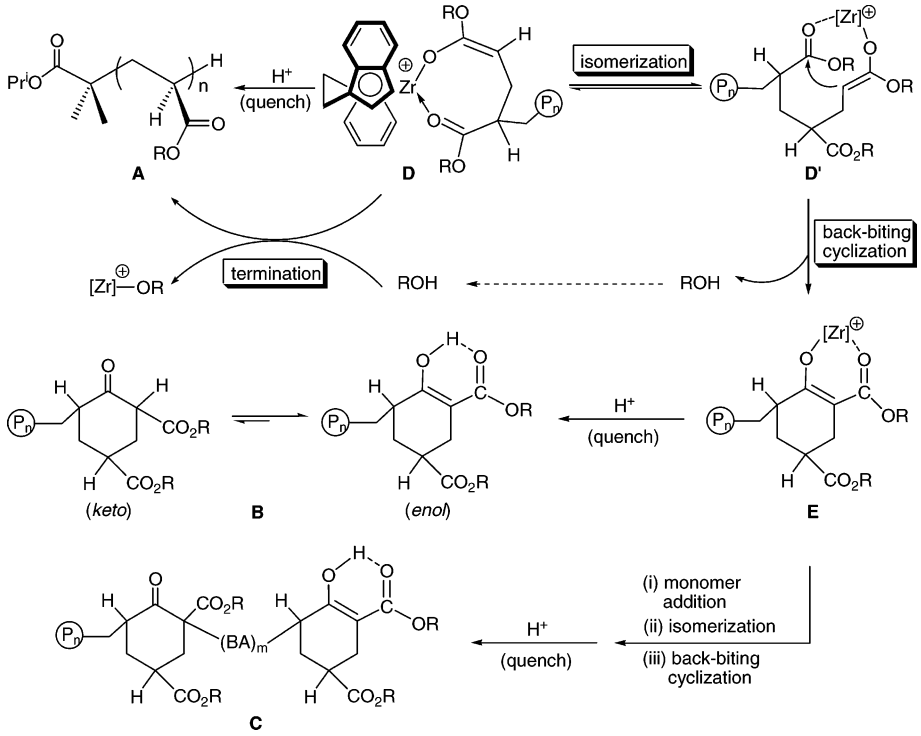

six-membered-ring zirconocenium β-ketoester enolate **E**, which is produced from intramolecular backbiting cyclizations involving the activated antepenultimate ester group of the growing polymer chain. Specifically, cyclic intermediate **E** and its coproduct ROH (R = ^{n}Bu in this example, Scheme 3) are formed by a single backbiting cyclization via ten-membered-ring cyclic ester enolate intermediate **D′**; this process requires ring-expansion isomerization of eight-membered-ring intermediate **D** to ten-membered ring homologue **D′**, allowing for more thermodynamically favorable formation of a six-membered-ring transition state for nucleophilic attack of the enolate carbon onto the antepenultimate ester carbonyl carbon. An intermolecular polymer termination involving intermediate **D** and a dead polymer chain is unlikely because this pathway would utilize the unactivated ester group of another polymer chain. Hydrolysis of **E** during the acidic workup procedure yields cyclic β-ketoester-terminated poly(*n*-BA) **B**, whereas the ROH formed from the backbiting cyclization deactivates the active propagating species **D** to give also linear chain **A** and the inactive zirconocenium alkoxide species. Further addition of *m* equiv of monomer to less reactive **E** (vs **D**) followed by a second backbiting cyclization gives the observed doubly cyclic β-ketoester-terminated poly(*n*-BA) **C** (after acidic workup) and also results in further catalyst deactivation.

Backbiting cyclization leading to a cyclic β-ketoester-terminated polyacrylate chain end (i.e., type **B** structure) is ubiquitous in the anionic polymerization of acrylates;[19] such a backbiting cyclization typically does not occur in the metallocene-mediated polymerization of methacrylates, presumably due to sterics at the α-C of the enolate moiety and the absence of the readily enolizable acidic α-proton (cf. structure **D′**). Increasing the steric protection of the carbonyl carbon of alkyl acrylates apparently does not play a measurable role in suppressing the backbiting cyclization in the current system because the polymerization of *tert*-butyl acrylate behaves similarly to that of the *n*-butyl acrylate polymerization. The acrylate-derived cyclic β-ketoester structure exists predominately in its enol form, and the proton of such an enol form in cyclic structures **B** or **C** produced in the current system can be readily identified in the ^{1}H NMR spectrum of the P(*n*-BA) produced with two small peaks at 12.21 and 12.46 ppm.[20,21] Reinitiation of a cyclic β-ketoester-terminated polyacrylate chain end (**B**-type structure) and subsequent formation of multiple cyclic β-ketoester-terminated polyacrylate chain ends (**C**-type structure) have been previously observed in the anionic polymerization of *n*-BA by a three-component system consisting of ethyl α-lithioisobutyrate/tetralkylammonium halide/trialkylaluminum.[22] What needs to be further confirmed in this overall mechanism, however, are the products of the backbiting cyclization and the reaction involving resting intermediate **D** and ROH.

The backbiting cyclization via intermediate **D′** could produce two possible product pairs, regardless how it occurs: (a) a cationic zirconocenium alkoxide complex and cyclic β-ketoester (**B**) pair or (b) a cationic zirconocenium cyclic β-ketoester enolate (**E**) and ROH pair. On the basis of pK_a values of the β-ketoester (~14) vs ROH (~30),[23] the **E**/ROH pair is expected

Scheme 4

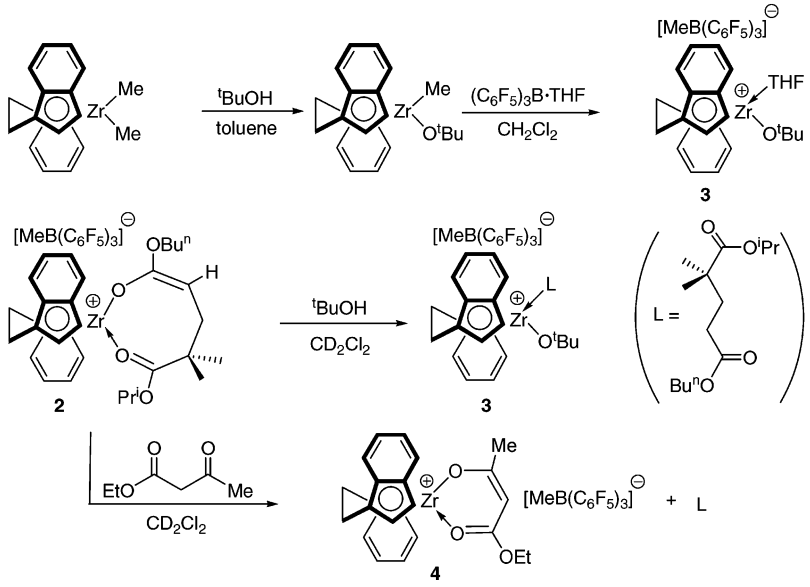

to be the thermodynamic products. To determine the products of the reaction between resting intermediate **D** and ROH, an authentic sample of cationic zirconocenium *tert*-butoxide complex **3** was prepared, and a model reaction was carried out (Scheme 4). Thus, treatment of the single *n*-BA addition product **2** (which models intermediate **D**) with ^{t}BuOH readily generates the cationic zirconocenium *tert*-butoxide complex **3**; a control experiment showed complex **3** to be inactive toward polymerization of *n*-BA over 24 h. Furthermore, to test whether zirconocenium cyclic β-ketoester enolate **E** can undergo further *n*-BA addition, or not, complex **2** was treated with ethyl acetoacetate (EAA) to generate in situ cyclic β-ketoester enolate **4** (as a model for structure **E**). Upon addition of 10 equiv of *n*-BA, **4** consumed only ~18% of the monomer within the initial 10 min without further monomer consumption over 24 h; this experiment implies that **E** is still active for *n*-BA addition, but it is much less active than **D**, satisfactorily accounting for the formation of a much smaller amount of doubly cyclic β-ketoester-terminated poly(*n*-BA), structure **C** (vs **B**).

Last, the termination mechanism proposed in Scheme 3 shows that linear chain **A** can be produced by either the post-polymerization acidic methanol quench of living intermediate **D** or in-polymerization termination of intermediate **D** by ^{n}BuOH generated from the backbiting cyclization, the latter process of which was demonstrated by the above model reaction. To show that the former process also contributes to the formation of **A**, the behavior of the block copolymerization starting out with *n*-BA and finishing with MMA was investigated. The hypothesis is that if the former process is operative, then there must be a fraction of the living propagating species (prior to workup) that is preserved and competent for initiation of MMA polymerization to yield a diblock copolymer at least at low $[n\text{-BA}]_0/[\mathbf{1}]_0$ ratios. Thus, after a polymerization of 20 equiv of *n*-BA by **1** in CH_2Cl_2 at 23 °C for 10 min, 200 equiv of MMA was added and allowed to react for 1 h, yielding a polymer product that contains ~10 mol % of the MMA units in 10% isolated polymer yield based on the total monomer feed. The content of the MMA units in the polymer product increased to ~39 mol % when the sequential copolymerization was carried out at 0 °C. Owing to substantial chain termination reactions during the polymerization of *n*-BA, the resulting polymer products have low molecular weights with multimodal GPC molecular weight distributions and are presumably mixtures of homopolymer P(*n*-BA) and block copolymer P(*n*-BA)-*b*-P(MMA). Furthermore, the unreacted *n*-BA in the first step substantially affects the polymerization of MMA in the second step. For example, in statistical copolymerizations of MMA and *n*-BA by **1**, only 1 mol % of *n*-BA in the feed significantly deactivates the catalyst, and 10 mol % of *n*-BA shuts down the polymerization! This phenomenon can be attributed to the facile termination via backbiting cyclization whenever the unhindered enolate is formed (i.e., when a *n*-BA molecule is enchained).[21] Although these complications prevented us from estimating the percentage of chains that are still living prior to workup, it is evident that at least a fraction of such living polymer chains contributes to the formation of structure **A** as a result of the workup quench. Overall, the results from the above analysis, model reaction, and polymerization studies are consistent with the overall chain termination mechanism shown in Scheme 3 for the acrylate polymerization by the current monometallic system.

Chain Transfer Reactions in the Acrylate Polymerization by 1. An investigation into reactions of the well-defined zirconocenium ester enolate complexes, including **1** and its single *n*-BA addition product **2**, with various types of enolizable esters, β-diesters, and β-ketoesters will not only provide direct evidence for possible chain transfer reactions but also shed light on whether certain types of enolizable esters could potentially serve as chain transfer reagents (CTRs) for the development of an efficient chain transfer polymerization of (meth)acrylates mediated by group 4 metallocene complexes. An important feature of the current monometallic propagating system is that the zirconocenium complex employed is bifunctional; it can be called either catalyst or initiator because a single complex serves as both initiator (containing the nucleophilic initiating group) and catalyst (activating the enchaining monomer via coordination). Thus, it is a catalyst when emphasizing the fundamental catalytic event of monomer enchainment, but it is not a "true" catalyst when the catalytic production of polymer chains is concerned. In efforts to transform zirconocene complexes into "true" catalysts, Carpentier and co-workers[24] investigated the feasibility of using enolizable ketones and thiols as CTRs—an approach that had been employed by Nodono et al.[25] to effect the chain transfer polymerization of MMA with organolanthanide complexes such as $(C_5Me_5)_2SmMe(THF)$—for MMA polymerization mediated by the $Cp_2ZrMe_2/B(C_6F_5)_3$ system. Thus, stoichiometric reactions of the cationic ester enolate

Scheme 5

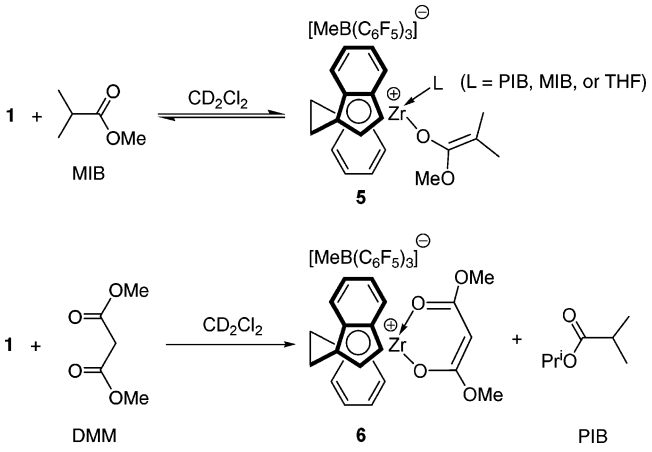

complex $[Cp_2Zr^+(THF)(O(^tBuO)C{=}CMe_2)][MeB(C_6F_5)_3]^-$ with these organic acids resulted in the formation of the undesired, inactive Zr-aldol product when enolizable ketones were used and the corresponding thiolates such as $[Cp_2Zr^+(S^tBu)(THF)][MeB(C_6F_5)_3]^-$ when thiols were employed. Although the resulting *tert*-butyl thiolate complex is still active for reinitiation of MMA polymerization, its poor initiation efficiency largely limited the effectiveness of ^{t}BuSH as a CTR in the MMA polymerization by the $Cp_2ZrMe_2/B(C_6F_5)_3$ system; hence, other types of organic acids are called for, in order to achieve effective chain transfer polymerization.

The equimolar reaction of **1** and methyl isobutyrate (MIB) in CD_2Cl_2 at ambient temperature resulted in the formation of an equilibrium mixture consisting of both the protonolysis product, *rac*-(EBI)Zr^+(L)[OC(OMe)=CMe_2][$MeB(C_6F_5)_3$]$^-$ (**5**, L = PIB, MIB, or THF, Scheme 5), and the starting materials in an approximate ratio of 1:2, with no noticeable change in this ratio after 5 h. On the other hand, monitoring the equimolar reaction of **1** with dimethyl malonate (DMM) in CD_2Cl_2 by ^{1}H NMR clearly shows the rapid disappearance of the peaks due to the starting materials and the appearance of a new set of resonances consistent with the formation of the corresponding protonolysis product, *rac*-(EBI)Zr^+[OC(OMe)=CHC(OMe)=O][$MeB(C_6F_5)_3$]$^-$ (**6**), and the readily identifiable free isopropyl isobutyrate (PIB) coproduct. The ^{1}H NMR spectrum of **6** exhibits an average C_2 symmetry in solution, suggesting a delocalized "acac"-type structure.

The above model reaction results also imply that enolizable esters such as MIB and DMM would not be suitable as effective chain transfer reagents for the polymerization of (meth)acrylates due to either inefficient chain transfer in the case of MIB or sluggish reinitiation in the case of DMM; to effect catalytic production of polymer chains, added CTRs must cleave or exchange the Zr−enolate bond (i.e., growing polymer chain) in a facile fashion on the polymerization time scale as well as efficiently reinitiate the polymerization. Indeed, the MMA polymerization by **1** in the presence of 1, 5, 10, 20, and 50 equiv (vs **1**) of MIB did not effect chain transfer polymerization. Within the MIB series, only small variations in activity with nearly constant [*mm*] (93%) and PDI (1.03) values as well as no change in M_n up to 20 equiv of MIB were observed. For the series of *β*-diesters (dimethyl-, diethyl-, and di-*tert*-butyl malonates), 10 equiv of CTR loadings resulted in diminished activity or complete shutting down of the polymerization, while at lower CTR loadings initiator efficiencies were much lower than expected for a chain transfer polymerization system.

Chain transfer reactions involving activation of protons in the α-position to the ester group of the polymer chain, the process indicated to be involved in the polymerization of *n*-BA by the bimetallic propagating system,[2k] were also considered in the current monometallic propagating system. Scheme 6 shows two possible pathways for proton-transfer involving the resting intermediate **D**: intramolecular proton shift to the enolate oxygen (i.e., formal cleavage of the Zr−enolate bond by the acidic α-proton) to give structure **F** and intermolecular proton transfer from a dead polymer chain to the enolate oxygen to give similar structure **G**, along with a release of a newly formed dead chain. In the intramolecular route, it is also possible other acidic α-protons further down the polymer chain can transfer the protons in the similar fashion, whereas in the intermolecular pathway, proton transfer involving two **D** molecules is less likely considering the sterics and charge repulsion between these two molecules. As compared to a tertiary α-C of the terminal ester enolate in structure **D**, the resulting structures **F** and **G** bear a quaternary α-C in the terminal (**F**) or internal (**G**) ester enolate moiety.

Scheme 6

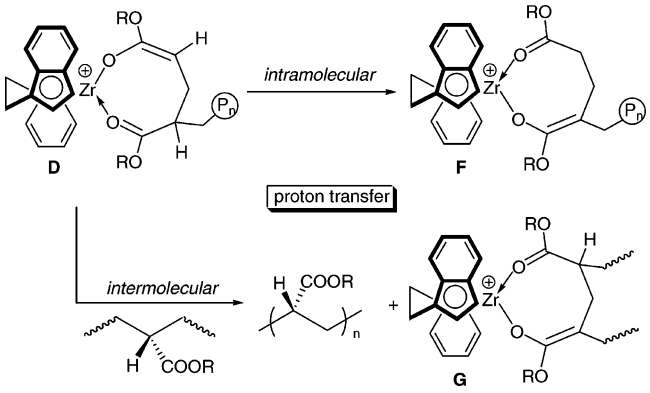

Structures **F** and **G** derived from proton transfer, if indeed formed on the polymerization time scale, could potentially exhibit different reactivity toward further chain growth from that of **D**. However, the reactivity of structure **F** should be comparable with that of **D** because structurally **F** is equivalent to **1** and thus **D**. Furthermore, structure **F** closely resembles that of the MMA propagating cyclic ester enolate structure **H** (Scheme 7) that is modeled by the isolated single-MMA-addition product,[3a] which has been shown to exhibit similar activity toward polymerization of *n*-BA to that obtained by complex **2** that models structure **D**. Specifically, after a complete consumption of 200 equiv of MMA by **1**, 100 equiv of *n*-BA was added to yield block copolymer product P(MMA)-*b*-P(*n*-BA) that contains 15 mol % of the *n*-BA units based on ^{1}H NMR; this composition corresponds to a 45% *n*-BA conversion, the value of which is consistent with that observed for the independent homopolymerization of 100 equiv of *n*-BA by **1** at 23 °C (i.e., 47%; run 3, Table 1). Extraction of the bulk polymer product with methanol at ambient temperature for extended times (≥12 h) resulted in a quantitative recovery of the insoluble polymer that has the same molar ratio of the MMA and *n*-BA units in the copolymer within experimental errors, confirming that it is the true copolymer product. (Note that low to medium molecular weight homopolymer P(*n*-BA) produced in this system is completely soluble in methanol.) The measured M_n and PDI of the copolymer product are 50K and 1.18, respectively, giving an overall initiator efficiency of ∼52% (based on 100% MMA and 45% *n*-BA conversions); this proportions to a ∼80% efficiency for the MMA polymerization[3a] and a ∼65% for the *n*-BA polymerization, again consistent with the independent homopolymerization of *n*-BA. There is a bimodal distribution of the obtained copolymer, however, as indicated by two sharp

Scheme 7

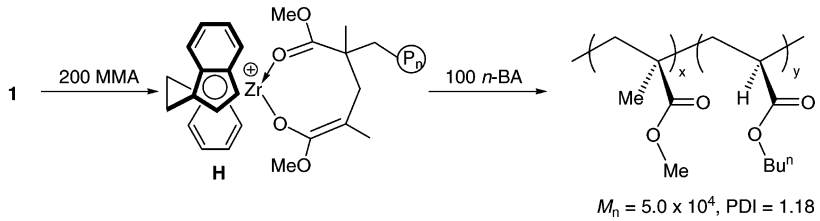

Table 2. MMA Polymerization Results by 1 in the Presence of DMS (as Dead Chain Model)[a]

run no.	MMA/DMS/**1** (molar ratio)	time (min)	temp (°C)	yield (%)	10^3M_n (g/mol)	PDI (M_w/M_n)	I^* (%)
1	500/1/1	30	23	92	56.8	1.03	81
2	500/5/1	30	23	88	55.6	1.03	80
3	500/10/1	30	23	88	57.5	1.03	77
4	500/20/1	30	23	87	56.4	1.04	77
5	500/50/1	30	23	86	58.3	1.11	74

[a] See Table 1 footnotes for explanations of the abbreviations listed in this table.

Scheme 8

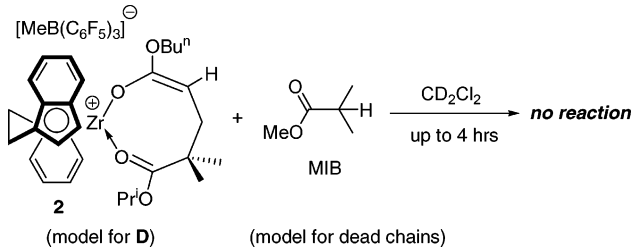

peaks (PDI = 1.04 for each peak) within a relatively broad overall peak (PDI = 1.18) on the GPC trace; the formation of this ill-defined block copolymer structure is anticipated due to the presence of the chain termination/transfer processes for the *n*-BA polymerization as described above. In short, the possible intramolecular proton transfer process, if indeed occurring in this monometallic system, should apparently neither deactivate the catalyst nor affect the apparent rate of further chain growth.

To directly assess the reactivity of the internally located ester enolate of structure **G** derived from the proposed intermolecular proton transfer (Scheme 6) remains a challenge because its reactivity is complicated by possible main chain mobility and entanglement issues. However, the model reaction between **1** and dimethyl succinate (DMS), a γ-diester, shows none to marginal reaction over a 14 h period; this is further backed by the results from the chain-transfer-type polymerization of MMA by **1** in the presence of various amounts of DMS. As can be seen from Table 2, addition of up to 50 equiv (vs **1**) of DMS neither deactivated the catalyst nor effected chain transfer polymerization, with only small variations in isolated polymer yield, M_n, PDI, and I^*. On the basis of these findings, it is evident that the possible intermolecular proton transfer in the current system appears to be too slow on the polymerization time scale (note that polymerization of *n*-BA is even faster than MMA) to affect chain transfer to polymer. If such chain transfer is facile relative to chain growth, polymer chain branching would occur. To provide additional support to the conclusion that proton transfer is insignificant in the current monometallic system, a model reaction directly relevant to the *n*-BA polymerization, outlined in Scheme 8, showed that there is no reaction between complex **2** (as a model for propagating intermediate **D**) and MIB (as a model for dead chain) for up to 4 h in a CD_2Cl_2 solution at ambient temperature (i.e., under polymerization conditions).

Conclusions

The well-defined monometallic propagating, chiral *ansa*-zirconocenium ester enolate complex **1** effects living polymerization of methacrylates and acrylamides; in sharp contrast, the polymerization of acrylates such as *n*-BA mediated by **1** proceeds in an uncontrolled fashion to only moderate conversions, producing P(*n*-BA) with one major linear structure **A** as well as two minor cyclic β-ketoester-terminated P(*n*-BA) structures **B** and **C**. Our investigations into polymerization characteristics, polymer chain structures, and model reactions have yielded unambiguous evidence for the presence of termination processes in this polymerization system that prevent it from achieving high monomer conversions and producing all living chains. The proposed overall three-step mechanism adequately explains these catalyst deactivation pathways and the resulting polymer chain structures. Some of the key features about this mechanism are summarized as follows.

First, isomerization of the eight-membered-ring zirconocenium ester enolate propagating species **D** (resting state) to its ten-membered-ring homologue **D′** followed by intramolecular backbiting cyclization involving the antepenultimate ester group of the growing polymer chain generates the much less active six-membered-ring zirconocenium β-ketoester enolate species **E** [which leads to cyclic β-ketoester-terminated **B** after acidic workup] and ^{n}BuOH. Second, the in situ eliminated ^{n}BuOH deactivates propagating species **D** to yield the inactive zirconocenium alkoxide species and linear chain **A**. Third, further addition of monomer to **E** followed by a second backbiting cyclization gives doubly cyclic β-ketoester-terminated **C** (after the acidic workup), accompanied by additional catalyst deactivation and chain termination as shown above. Overall, the lack of steric protection at the unhindered α-C of the ester enolate moiety in the propagating species facilitates the backbiting cyclization, whereas the active (readily enolizable) α-proton provides access for elimination of ^{n}BuOH that subsequently terminates the chain.

Model reactions and polymerization studies show that possible chain transfer reactions involving acidic α-protons are insignificant as compared with backbiting cyclizations in the current monometallic catalyst system. With the catalyst deactivation pathways being identified and the mechanism of which understood, it is envisioned that strategies, such as prevention of isomerization of the active cyclic ester enolate resting state by virtue of ligand design, can be developed to overcome these side reactions and thus render a living/controlled polymerization of acrylates mediated by group 4 metallocene catalysts.

Acknowledgment. Funding for this work was provided by the National Science Foundation and Colorado State University. We thank Boulder Scientific Co. for the gift of $B(C_6F_5)_3$ and the reviewers for their valuable comments and suggested additional experiments. The A.P. Sloan Foundation (Research Fellowship to E.Y.C.) and ARCS/Hach Foundation (Graduate Fellowship to W.R.M.) are gratefully acknowledged.

CDV

References and Notes

(1) (a) Collins, S.; Ward, S. G. *J. Am. Chem. Soc.* **1992**, *114*, 5460−5462. (b) Yasuda, H.; Yamamoto, H.; Yokota, K.; Miyake, S.; Nakamura, A. *J. Am. Chem. Soc.* **1992**, *114*, 4908−4909. (c) Farnham, W. B.; Hertler, W. U.S. Pat. 4,728,706, 1988.

(2) (a) Kostakis, K.; Mourmouris, S.; Kotakis, K.; Nikogeorgos, N.; Pitsikalis, M.; Hadjichristidis, N. *J. Polym. Sci., Part A: Polym. Chem.* **2005**, *43*, 3305−3314. (b) Stojcevic, G.; Kim, H.; Taylor, N. J.; Marder, T. B.; Collins, S. *Angew. Chem., Int. Ed.* **2004**, *43*, 5523−5526. (c) Lian, B.; Toupet, L.; Carpentier, J.-F. *Chem.—Eur. J.* **2004**, *10*, 4301−4307. (d) Ferenz, M.; Bandermann, F.; Sustmann, R.; Sicking, W. *Macromol. Chem. Phys.* **2004**, *205*, 1196−1205. (e) Karanikolopoulos, G.; Batis, C.; Pitsikalis, M.; Hadjichristidis, N. *J. Polym. Sci., Part A: Polym. Chem.* **2004**, *42*, 3761−3774. (f) Wang, J.; Odian, G.; Haubenstock, H. *Polym. Prepr.* **2003**, *44*, 673−674. Wang, J.; Haubenstock, H.; Odian, G. *Polym. Prepr.* **2003**, *44*, 675−676. (g) Bandermann, F.; Ferenz, M.; Sustmann, R.; Sicking, W. *Macromol. Symp.* **2001**, *174*, 247−253. (h) Karanikolopoulos, G.; Batis, C.; Pitsikalis, M.; Hadjichristidis, N. *Macromolecules* **2001**, *34*, 4697−4705. (i) Bandermann, F.; Ferenz, M.; Sustmann, R.; Sicking, W. *Macromol. Symp.* **2000**, *161*, 127−134. (j) Shiono, T.; Saito, T.; Saegusa, N.; Hagihara, H.; Ikeda, T.; Deng, H.; Soga, K. *Macromol. Chem. Phys.* **1998**, *199*, 1573−1579. (k) Li, Y.; Ward, D. G.; Reddy, S. S.; Collins, S. *Macromolecules* **1997**, *30*, 1875−1883. (l) Deng, H.; Shiono, T.; Soga, K. *Macromol. Chem. Phys.* **1995**, *196*, 1971−1980.

(3) (a) Rodriguez-Delgado, A.; Chen, E. Y.-X. *Macromolecules* **2005**, *38*, 2587−2594. (b) Bolig, A. D.; Chen, E. Y.-X. *J. Am. Chem. Soc.* **2004**, *126*, 4897−4906. (c) Strauch, J. W.; Fauré, J.-L.; Bredeau, S.; Wang, C.; Kehr, G.; Fröhlich, R.; Luftmann, H.; Erker, G. *J. Am. Chem. Soc.* **2004**, *126*, 2089−2104. (d) Chen, E. Y.-X.; Cooney, M. J. *J. Am. Chem. Soc.* **2003**, *125*, 7150−7151. (e) Karanikolopoulos, G.; Batis, C.; Pitsikalis, M.; Hadjichristidis, N. *Macromol. Chem. Phys.* **2003**, *204*, 831−840. (f) Batis, C.; Karanikolopoulos, G.; Pitsikalis, M.; Hadjichristidis, N. *Macromolecules* **2003**, *36*, 9763−9774. (g) Bolig, A. D.; Chen, E. Y.-X. *J. Am. Chem. Soc.* **2002**, *124*, 5612−5613. (h) Frauenrath, H.; Keul, H.; Höcker, H. *Macromolecules* **2001**, *34*, 14−19. (i) Bolig, A. D.; Chen, E. Y.-X. *J. Am. Chem. Soc.* **2001**, *123*, 7943−7944. (j) Cameron, P. A.; Gibson, V.; Graham, A. J. *Macromolecules* **2000**, *33*, 4329−4335. (k) Stuhldreier, T.; Keul, H.; Höcker, H. *Macromol. Rapid Commun.* **2000**, *21*, 1093−1098. (l) Chen, Y.-X.; Metz, M. V.; Li, L.; Stern, C. L.; Marks, T. J. *J. Am. Chem. Soc.* **1998**, *120*, 6287−6305. (m) Deng, H.; Shiono, T.; Soga, K. *Macromolecules* **1995**, *28*, 3067−3073. (n) Soga, K.; Deng, H.; Yano, T.; Shiono, T. *Macromolecules* **1994**, *27*, 7938−7940. (o) Collins, S.; Ward, D. G.; Suddaby, K. H. *Macromolecules* **1994**, *27*, 7222−7224.

(4) Saegusa, N.; Shiono, T.; Ikeda, T.; Mikami, K. JP 10330391, 1998.

(5) (a) Jin, J.; Mariott, W. R.; Chen, E. Y.-X. *J. Polym. Chem., Part A: Polym. Chem.* **2003**, *41*, 3132−3142. (b) Jin, J.; Chen, E. Y.-X. *Organometallics* **2002**, *21*, 13−15.

(6) (a) Chen, E. Y.-X. *J. Polym. Sci., Part A: Polym. Chem.* **2004**, *42*, 3395−3403. (b) Jensen, T. R.; Yoon, S. C.; Dash, A. K.; Luo, L.; Marks, T. J. *J. Am. Chem. Soc.* **2003**, *125*, 14482−14494.

(7) (a) Rodriguez-Delgado, A.; Mariott, W. R.; Chen, E. Y.-X. *Macromolecules* **2004**, *37*, 3092−3100. (b) Jin, J.; Chen, E. Y.-X. *Macromol. Chem. Phys.* **2002**, *203*, 2329−2333. (c) Jin, J.; Wilson, D. R.; Chen, E. Y.-X. *Chem. Commun.* **2002**, 708−709. (d) Nguyen, H.; Jarvis, A. P.; Lesley, M. J. G.; Kelly, W. M.; Reddy, S. S.; Taylor, N. J.; Collins, S. *Macromolecules* **2000**, *33*, 1508−1510.

(8) (a) Hölscher, M.; Keul, H.; Höcker, H. *Macromolecules* **2002**, *35*, 8194−8202. (b) Hölscher, M.; Keul, H.; Höcker, H. *Chem.—Eur. J.* **2001**, *7*, 5419−5426. (c) Sustmann, R.; Sicking, W.; Bandermann, F.; Ferenz, M. *Macromolecules* **1999**, *32*, 4204−4213.

(9) Deng, H.; Soga, K. *Macromolecules* **1996**, *29*, 1847−1848.

(10) Kostakis, K.; Mourmouris, S.; Pitsikalis, M.; Hadjichristidis, N. *J. Polym. Sci., Part A: Polym. Chem.* **2005**, *43*, 3337−3348.

(11) Ihara, E.; Morimoto, M.; Yasuda, H. *Macromolecules* **1995**, *28*, 7886−7892.

(12) The Ziegler group at the University of Calgary informed us of their ongoing computational study of the polymerization of acrylates by monometallic cationic zirconocenes; we thank Dr. Simone Tomasi for helpful discussions.

(13) (a) Mariott, W. R.; Chen, E. Y.-X. *Macromolecules* **2005**, *38*, 6822−6832. (b) Mariott, W. R.; Chen, E. Y.-X. *Macromolecules* **2004**, *37*, 4741−4743.

(14) Allen, R. D.; Long, T. E.; McGrath, J. E. *Polym. Bull. (Berlin)* **1986**, *15*, 127−134.

(15) (a) Grossman, R. B.; Doyle, R. A.; Buchwald, S. L. *Organometallics* **1991**, *10*, 1501−1505. (b) Collins, S.; Kuntz, B. A.; Taylor, N. J.; Ward, D. G. *J. Organomet. Chem.* **1988**, *342*, 21−29.

(16) Diamond, G. M.; Jordan, R. F.; Petersen, J. L. *J. Am. Chem. Soc.* **1996**, *118*, 8024−8033.

(17) (a) Stoebenau, E. J., III; Jordan, R. F. *J. Am. Chem. Soc.* **2003**, *125*, 3222−3223. (b) Hong, Y.; Kuntz, B. A.; Collins, S. *Organometallics* **1993**, *12*, 964−969.

(18) (a) Kawamura, T.; Toshima, N.; Matsuzaki. *Macromol. Chem. Phys.* **1995**, *196*, 3415−3424. (b) Bovey, F. A.; Mirau, P. A. *NMR of Polymers*; Academic Press: San Diego, 1996. (c) Ferguson, R. C.; Ovenall, D. W. *Macromolecules* **1987**, *20*, 1245−1248. (d) Ferguson, R. C.; Ovenall, D. W. *Polym. Prepr.* **1985**, *26*, 182−183. (e) Subramanian, R.; Allen, R. D.; McGrath, J. E.; Ward, T. C. *Polym. Prepr.* **1985**, *26*, 238−240.

(19) For a recent review, see: Baskaran, D. *Prog. Polym. Sci.* **2003**, *28*, 521−581.

(20) Tabuchi, M.; Kawauchi, T.; Kitayama, T.; Hatada, K. *Polymer* **2002**, *43*, 7185−7190.

(21) Jacobs, C.; Varshney, S. K.; Hautekeer, J.-P.; Fayt, R.; Jérôme, R.; Teyssié, P. *Macromolcules* **1990**, *23*, 4024−4025.

(22) Schmitt, B.; Müller, A. H. E. *Macromolecules* **2001**, *34*, 2115−2120.

(23) Bordwell, F. G. *Acc. Chem. Res.* **1988**, *21*, 456−463.

(24) Lian, B.; Lehmann, C. W.; Navarro, C.; Carpentier, J.-F. *Organometallics* **2005**, *24*, 2466−2472.

(25) Nodono, M.; Tokimitsu, T.; Tone, S.; Makino, T.; Yanagase, A. *Macromol. Chem. Phys.* **2000**, *201*, 2282−2288.

MA052305+